RSC Advances

This is an *Accepted Manuscript*, which has been through the Royal Society of Chemistry peer review process and has been accepted for publication.

Accepted Manuscripts are published online shortly after acceptance, before technical editing, formatting and proof reading. Using this free service, authors can make their results available to the community, in citable form, before we publish the edited article. This *Accepted Manuscript* will be replaced by the edited, formatted and paginated article as soon as this is available.

You can find more information about *Accepted Manuscripts* in the Information for Authors.

Please note that technical editing may introduce minor changes to the text and/or graphics, which may alter content. The journal's standard Terms & Conditions and the Ethical guidelines still apply. In no event shall the Royal Society of Chemistry be held responsible for any errors or omissions in this *Accepted Manuscript* or any consequences arising from the use of any information it contains.

ROYAL SOCIETY OF CHEMISTRY

www.rsc.org/advances

Enhanced gas sensing properties of V_2O_5 nanowires decorated with SnO_2 nanoparticles to ethanol at room temperature

Ruibing Wang[a,†], Shuang Yang[a,†], Rong Deng[a], Wen Chen[a], Yueli Liu [a,*], Han Zhang[b], Galina S. Zakharova[c]

[a] State Key Laboratory of Advanced Technology for Materials Synthesis and Processing, School of Materials Science and Engineering, Wuhan University of Technology, Wuhan 430070, P. R. China

[b] Key Laboratory of Optoelectronic Devices and Systems of Ministry of Education and Guangdong Province, Shenzhen University, 518060, P. R. China

[c] Institute of Solid State Chemistry, Ural Branch of the Russian Academy of Science, Ekaterinburg 620990, Russian Federation

[*] Correspondent:

Prof. Yueli LIU

Tel.: +86-27-87760159

Fax: +86-27-87760129

E-mail: **lylliuwhut@whut.edu.cn (Yueli LIU)**

[†] These authors contributed equally to this study and share first authorship.

RSC Advances Accepted Manuscript

Abstract

V_2O_5 nanowires decorated with SnO_2 nanoparticles are prepared by two-step mild hydrothermal reaction, and the gas sensor device is fabricated by coating the nanowires as a thick film on the alumina tube. The pure V_2O_5 nanowires have almost no response to ethanol at room temperature, however, the sensitivity of V_2O_5 nanowires decorated with SnO_2 nanoparticles is 1.46 upon exposure to 1000 ppm ethanol gas. The highest sensitivity of gas sensor based on V_2O_5 nanowires decorated with SnO_2 nanoparticles to 1000 ppm ethanol is about 16, which is 2-3 times of pure V_2O_5 nanowires. The improved sensing performance of the composite is due to the increased depletion width and active sites along the nanowires, moreover, the energy gap between V_2O_5 nanowires and SnO_2 nanoparticles promotes the electrons transport. Moreover, the gas sensor based on V_2O_5 nanowires decorated with SnO_2 nanoparticles possesses a good selectivity to ethanol compared with other gases, such as CO_2, H_2O and NH_3, and the stability of gas sensing performance is quite good, which implies that it would be a good candidate in the potential application.

RSC Advances Accepted Manuscript

1. Introduction

With the increasing awareness of human health and security, alcohol sensors have been in great demand in the biomedical, chemical, wine quality monitoring and breathe analysis applications. Nowadays, resistive gas sensors based on metal oxide semiconductor materials have become a hot research area and occupied more than 60% market share due to their ease of use, real-time detection, high sensitivity and low cost.[1-7]

At present, semiconductors including SnO_2, ZnO and Fe_2O_3 are mostly used for the detection of ethanol vapor. However, the poor selectivity and high working temperature limit their application and further exploration of new materials is needed.[2-3] Vanadium pentoxide (V_2O_5) has attracted considerable interest owing to its unique layered structure and various valence states like V^{5+}, V^{4+} and V^{3+}.[4-6] Having the large specific surface area and character of electrons transmission along axis direction, one-dimensional (1-D) structured V_2O_5 may have an even promising future in the application of gas sensor. Raible *et al.* fabricated gas sensors by depositing V_2O_5 nanofibres from aqueous suspension onto the silicon substrates and tested the gas sensing properties to amines.[7] The sensors could be operated at room temperature, and the extremely high sensitivity for 1-butylamine (limit of detection (LOD) below 30 ppb) and moderate sensitivity for ammonia were obtained. However, very little sensitivity was observed for toluene and 1-propanol vapors. Yu *et al.* prepared gas nanodevices based on V_2O_5 nanowires to helium gas and environmental pressures,[8] and the electrical response to helium was due to the physical adsorption of the helium

RSC Advances Accepted Manuscript

atoms into the interlayer of V_2O_5 nanowires. Liu *et al.* prepared curly V_2O_5 nanobelts via a simple mild hydrothermal method and tested the gas sensing properties to ethanol, H_2S, NH_3, H_2, C_3H_8, CO and NO_x,[9] and the sensors based on V_2O_5 nanobelts had a good response to ethanol in a wide range of 150-400 ˚C, and it was found that the layered structure would allow gas molecules to insert and approach the active position easily. Modafferi *et al.* reported a kind of highly sensitive resistive sensor based on electrospun V_2O_5 fibers to ammonia, it could response to ammonia at the temperature range from 50 ˚C to 300 ˚C, and the detection limit was about 100 ppb at 200 ˚C.[10]

Although V_2O_5 nanowires have excellent gas sensing properties according to the reports, which may make them an ideal candidate for gas sensor. However, there are few reports focused on V_2O_5 nanowires based gas sensor in recent years. The limited maximum sensitivity performance and high operating temperature might be the reasons that limit their real application.[11] The solutions to improve the sensitivity as well as decrease operating temperature in literature focus on controlling the morphology,[12] element doping[13] and decorating with different semiconductor metal oxides.[14-16] Decorating with different semiconductor metal oxides is an effective choice due to the advantage of the simple progress, low cost, high yield, and so forth.

Among them, tin dioxide (SnO_2) is an attractive sensing material due to its high electrical conductivity, wide-band gap and excellent chemical stability.[17-20] SnO_2 nanoparticles are on of the most applied sensing materials, which have been used to fabricate gas sensors to C_2H_5OH, ammonia (NH_3), H_2, CH_4, H_2O and so on. In

RSC Advances Accepted Manuscript

particular, SnO_2 nanoparticles are widely used for an additive as well, and they show excellent performance at improving the gas sensing properties of the base materials.[21-22] Chen reported the significant enhancement of CuO nanowire gas sensing performance at room temperature through the surface functionalization with SnO_2 nanocrystals,[23] and the sensitivity enhancement could be as high as 300 % for detecting 1% NH_3 diluted in air. Zhang prepared SnO_2 nanoparticles-reduced graphene oxide (SnO_2-RGO) nanocomposites via hydrothermal treatment.[24] It was found that SnO_2-RGO nanocomposites exhibit high response of 3.31 to 5 ppm NO_2 at 50 °C, which was much higher than that of RGO (1.13). The SnO_2-RGO nanocomposites also improved the sensing properties like rapid response, good selectivity and reproducibility. Therefore, it is still needed to enrich the works on the enhanced gas sensitivity by decorated with SnO_2 nanoparticles.

In this study, V_2O_5 nanowires are prepared via hydrothermal reaction and then decorated with SnO_2 nanoparticles. The gas sensing behavior to ethanol gas is tested at the temperature ranges from room temperature to 380 °C, and the influence of the decorated SnO_2 nanoparticles on the improved gas sensing behavior is also discussed.

2. Experimental section

2.1 Materials synthesis

Two steps were employed to prepare the SnO_2 nanoparticles decorated V_2O_5 nanowires. Firstly, the V_2O_5 sols were prepared by melt quenching method.[25] In the typical process, V_2O_5 powder was melted at 800 °C for 30 min and then poured into deionized water under vigorous stirring. The above obtained sols were transferred into

RSC Advances Accepted Manuscript

an autoclave and kept at 200 °C for 4 days. After the hydrothermal reaction, an orange and viscous solution of the V_2O_5 nanowires was obtained. The viscous solution was washed with ethanol and distilled water several times. Then the nanowires were dried at 80 °C in vacuum for 12 h for future use. Secondly, the nanowires were dispersed uniformly in 40 mL deionized water to form a 2.5 mmol/L solution (solution A). Then $SnCl_4$ powder was dissolved in deionized water, and the concentration of the solution was fixed to be 0.1 mmol/L (solution B). 1 mL solution B was dropwise added into solution A and kept stirring for 3 hours. After that, a second hydrothermal reaction was carried out at 100 °C for 6, 12 and 18 hours to obtain SnO_2 nanoparticles decorated V_2O_5 nanowires.

2.2 Characterization

The morphology and structure of as-prepared samples were characterized with an X-ray diffractometer (D/MAX-III) using a Cu Kα radiation and graphite monochromator, a field emission scanning electron microscopy (FESEM) at 5 kV (Hitachi S-4800), a transmission electron microscope (TEM) at 200 kV (JEOL, JEM-2100 TEM), and the element analysis is characterized by energy-dispersive X-ray (EDAX) (EDAX, EDX Genesis XM) equipped in the field emission scanning electron microscopy.

2.3 Sensor fabrication and sensing response measurement

Sensors based on V_2O_5 nanowires decorated with SnO_2 nanoparticles are fabricated by using alumina tubes. The schematic of alumina tube and its operating mechanism is shown in Fig. 1. Its length, internal diameter and external diameter are

RSC Advances Accepted Manuscript

4.0 mm, 1.0 mm in and 1.4 mm, respectively, and the Au electrodes with Pt lead wires are about 2.0 mm in distance. When fabricating a sensor, nanowires are firstly coated onto the alumina tube until it is wholly covered on the surface to form a sensing layer, and then the sensing layer is dried at 60 °C. In order to compare among different sensors, the weight of sensing layer should be controlled as the same (0.2 mg). Finally, a Ni–Cr heating wire is inserted into the tube for heating and the sensor is aged at 400 °C for 2 h. The gas sensing properties are characterized using a commercial gas sensing measurement system of WS-30A (ZhengZhou WeiSheng Corp.). The target gases are ethanol, CO_2, H_2O and NH_3 in dry air, and the ethanol gas is obtained by evaporating a certain volume of ethanol liquid on the heater plate of the machine. The response of sensor to testing gases (S) is determined by the relative resistance. For n-type gas sensors, the sensitivity is defined as $S = R_a/R_g$ when the target gas is reducing gas, and $S = R_g/R_a$ when the target gas is oxidizing gas, where R_a is the resistance of a sensor in air and R_g is the resistance of a sensor in a testing gas.

3. Results and discussion

The length of V_2O_5 nanowires is more than dozens of micron meters, the V_2O_5 nanowires are 50-100 nm in diameter in Fig. 2. Fig. 3 shows the FESEM images of pure V_2O_5 nanowires and V_2O_5 nanowires decorated with SnO_2 nanoparticles, which are synthesized after different hydrothermal times. As one can see, the shape of nanowires is totally remained and the surfaces of the nanowires are rough after a second hydrothermal reaction. The sizes of the SnO_2 nanoparticles on V_2O_5 nanowires increase with the increasing of hydrothermal time. The XRD patterns of the V_2O_5

RSC Advances Accepted Manuscript

nanowires and V_2O_5 nanowires decorated with SnO_2 nanoparticles are shown in Fig. 4, and it is observed that all the diffraction peaks of pure V_2O_5 nanowires are in good agreement with the orthorhombic V_2O_5 phase (JCPDS 089-2482). The diffraction peaks from SnO_2 phase are not found in XRD pattern because of the low amount in the product, as the amounts of V_2O_5 and $SnCl_4$ in the precursor are 0.1 mmol V_2O_5 and $0.1*10^{-3}$ mmol $SnCl_4$ in our case, respectively and the existence of the SnO_2 nanoparticles is needed to be further proved by EDS pattern and HRTEM image.

Fig. 5 (a) shows the EDS pattern of V_2O_5 nanowires decorated with SnO_2 nanoparticles prepared after hydrothermal times of 12 h, and it shows that the Sn content in the sample is about 0.08At%, which is almost match with the ratio of the precursor of $SnCl_4$. Combined with the scanning SEM image in Fig. 5 (b) and EDS elemental mapping (Figure 6 (c-e)), the current result reveals that the sample is composed of three elements of O, V and Sn, which confirm the formation of SnO_2 phase in the V_2O_5 nanowires decorated with SnO_2 nanoparticles.

Fig. 6 (a-d) show the TEM images of the pure V_2O_5 nanowires and SnO_2 decorated V_2O_5 nanowires prepared after different hydrothermal times. It shows that the surface of pure V_2O_5 nanowires (V_2O_5 NWs) before decoration is smooth without anything grown on it. However, the TEM images of V_2O_5 nanowires decorated with SnO_2 nanoparticles prepared after hydrothermal times of 6 h, 12 h and 18 h show that there are nanoparticles on the surface of the nanowires. The particles are randomly separated on the surface when the hydrothermal time is 6 h, and the particles are uniformly separated on the surface when the hydrothermal time is 12 h. When the

RSC Advances Accepted Manuscript

hydrothermal time is 18 h, there are too much particles on the surface that they begin to be agglomerate. The HRTEM image of sample prepared after hydrothermal time of 12 h is shown in Fig. 6(e), the marked values of 0.35 nm and 0.37 nm correspond to inter-planar *d*-spacing of the (210) and (110) lattice planes of the orthorhombic V_2O_5 and SnO_2, respectively, which further approves that the good crystallization of the SnO_2 nanoparticles on the V_2O_5 nanowires, and it is accord with the EDS results in Fig. 5.

Fig. 7 (a-h) shows the sensitivity of the sensors based on V_2O_5 nanowires and samples prepared after hydrothermal times of 6, 12 and 18 h to different concentrations of ethanol gas, and the operating temperature ranges from 60 to 380 ˚C. It is observed that all the sensors have a response to ethanol gas in the range of 10-1000 ppm and operates a good reversibility. Sensor based on SnO_2 decorated V_2O_5 nanowires show higher sensitivity compared with that based on pure V_2O_5 and SnO_2 decorated V_2O_5 nanowires prepared after hydrothermal times of 12 h show the highest sensitivity in the whole range of operating temperature.

Fig. 8 (a) shows the sensitivity of sensors based on V_2O_5 nanowires, SnO_2 nanoparticles and V_2O_5 nanowires decorated with SnO_2 nanoparticles prepared after hydrothermal times of 6, 12 and 18 h to 1000 ppm ethanol at various temperatures. V_2O_5 nanowires decorated with SnO_2 nanoparticles show the best response, however, the highest sensitivity appears at the same temperature of 332 ˚C. The result shows that the formation of the composite does not change its optimum working temperature of 332 ◦C, which is accord with some others' work. [26-27]As the decoration of SnO_2

RSC Advances Accepted Manuscript

nanoparticle could favor to increase the depletion layer and exposure more active sites to react with the target gas, which may increase the sensitivity as shown in Fig. 7. However, the operating temperature is related with the reaction energies and activation energy between ethanol molecules and the sensing layer,[28] and they are influenced by the kinds, morphologies and surface states and the energy structures of the sensing materials.[29-30] Therefore, we think that the reason lies in the fact that the content of SnO_2 nanoparticles in V_2O_5 nanowires decorated with SnO_2 nanoparticles is too small, and it would not have an obvious change for the operating temperature.

Fig. 8 (b) shows the value of sensitivity to ethanol at 60 ˚C among sensors based on SnO_2 nanoparticles, pure V_2O_5 nanowires and V_2O_5 nanowires decorated with SnO_2 nanoparticles prepared after hydrothermal times of 6, 12 and 18 h. It is obvious to see that sensor based on pure V_2O_5 nanowires have almost no response to ethanol at 60 ˚C , but sensors based on V_2O_5 nanowires decorated with SnO_2 nanoparticles prepared after hydrothermal times of 6, 12 and 18 h could have a great improvement in sensitivity. When the ethanol concentration is 1000 ppm, the sensitivity of V_2O_5 nanowires decorated with SnO_2 nanoparticles prepared after hydrothermal time of 12 h to ethanol is about 2.7, which is 1.8 times of the sensitivity of SnO_2 particles. The operating temperature of V_2O_5 gas sensors are commonly in the range of 200-400 ˚C in reported works, which may be a potential problem for the lifetime and safety of the gas sensor devices. In our case, the excellent ability of gas sensing response at low operating temperature suggests that the present gas sensor may possess a longer device lifetime, better device safety and lower energy consumption. Therefore, the

RSC Advances Accepted Manuscript

above special advantages may favor for their further applications.

V_2O_5 nanowires decorated with SnO_2 nanoparticles prepared after hydrothermal time of 12 h even has a response to 10-1000 ppm ethanol gas at room temperature (Fig. 8 (c)). In the concentration range of 10-500 ppm, the sensitivity value increase with the ethanol concentration. However, the sensitivity value shows a decreasing when the concentration is 1000 ppm, which may suggest that the sensor based on V_2O_5 nanowires decorated SnO_2 nanoparticles prepared after the hydrothermal time of 12 h have a maximum detection limit of 500 ppm at room temperature.[31] As ethanol could not be desorbed easily at room temperature, when the concentration of testing gas is too high, it may fail to be desorbed absolutely from the surface and the undesorbed ethanol molecules may occupy the active sites.[32] Therefore, the amount of ethanol molecules is too high to be absolutely desorbed on the surface at room temperature after testing 500 ppm ethanol. When testing 1000 ppm ethanol gas, although the concentration of target gas increases, the sites that have absorbed ethanol molecules in could not absorb more ethanol molecules. Therefore, the total amount of gas adsorption is decreased actually. In this case, we suggest that the poor desorb ability in high gas concentration is the reason that the sensitivity value to 1000 ppm ethanol is lower than that of 500 ppm at room temperature, and study of the absorb/desorb mechanism is to be carried out in future work. The selectivity and stability properties are important for a gas sensor.[33] In our work, the selectivity and stability properties of sensor based on V_2O_5 nanowires decorated with SnO_2 nanoparticles prepared after hydrothermal time of 12 h are also tested, which are

RSC Advances Accepted Manuscript

shown in Fig. 9. When the sensor based on V_2O_5 nanowires decorated with SnO_2 nanoparticles prepared after hydrothermal time of 12 h is exposed in C_2H_5OH, CO_2, H_2O and NH_3, it shows good response to C_2H_5OH and almost no response towards other target gases. The stability of sensors in 6 days shows that the value of sensitivity stay at the value of about 13, which shows that the present gas sensor has a good stability under long working time.

There might be three points that lead to the improvement of gas sensing properties of SnO_2 nanoparticles decorated V_2O_5 nanowires. Firstly, the decorated SnO_2 nanopaticles would favor for the increasing of the depletion layer and exposure more active sites to react with the target gas (Fig. 10).[34] Therefore, SnO_2 nanopaticles modified V_2O_5 nanowires would have a larger change in resistance when exposed to the target gas, which finally results in the improvement of gas sensing response. [35] Secondly, the energy level of SnO_2 conduction band (-4.5 eV) is a little higher than that of V_2O_5 (-4.6 eV). When the ethanol molecule is captured on the surface of SnO_2 nanopaticles, electrons are generated in the conduction band, and then the electrons will quickly transport to the conduction band of V_2O_5 (Fig. 11).[36] Thirdly, in a simplistic approximation, inter-contact between the nanowires are normally described as a high resistive barriers, which represents the main contribution to the overall resistance of the gas sensor device. As the special geometric structure of the nanowires, it could provide a direct path for electron transfer along the nanowire axis to shorten the inter-contacts between the nanowires (Fig. 12). Thus, after the decoration of SnO_2 nanoparticles, the existence of SnO_2 nanoparticles would firstly

RSC Advances Accepted Manuscript

favor to absorb more oxygen molecules and form thicker depletion layer. Then more electrons could be released to the conduction band of V_2O_5 nanowires when the sensor is exposed to the reducing gas. Finally, the electrons transport along the nanowire axis efficiently due to the special advantage of ultralong V_2O_5 nanowires. As a result, V_2O_5 nanowires decorated with SnO_2 nanoparticles show a better gas sensing response than that of pure V_2O_5 nanowires and SnO_2 nanoparticles.

4. Conclusions

In summary, SnO_2 decorated V_2O_5 nanowires are prepared and their gas sensing characteristics to ethanol are examined. The XRD patterns and FESEM images suggest that V_2O_5 nanowires with SnO_2 nanopaticles evenly dispersed on the surface could be obtained after hydrothermal time of 12 h. The gas responses was significantly improved after the decoration with SnO_2 nanoparticles, the sensitivity of SnO_2 decorated V_2O_5 nanowires at the hydrothermal time of 12 h to 1000 ppm ethanol is about 2-3 times higher than that of pure V_2O_5 nanowires. SnO_2 nanoparticles decorated V_2O_5 nanowires would even have a response to 10 ppm ethanol at room temperature. The improved gas sensing performance of the composite is due to the increased depletion width and active sites along the nanowires, the formation of heterojunction and the reducing of contact effects between the nanowires.

Acknowledgements

This work is supported by International Science & Technology Cooperation Program of China (No. 2013DFR50710), Equipment pre-research project (No.

RSC Advances Accepted Manuscript

625010402), Science and Technology Support Program of Hubei Province (No. 2014BAA096), the National Nature Science Foundation of Hubei Province (No. 2014CFB165), Ministry of Education and Science of Russia (No. 14.613.21.0002), and the Key Laboratory of Optoelectronic Devices and Systems of Ministry of Education and Guangdong Province (No. GD201402).

RSC Advances Accepted Manuscript

References

[1] J. Kong, N. R. Franklin, C. Zhou, M. G. Chapline, S. Peng, K. Cho and H. Dai, *Science*, 2000, **287**, 622.

[2] B. Y. Wei, M. C. Hsu, P. G. Su, H. M. Lin, R. J. Wu and H. J. Lai, *Sens. Actuators B*, 2004, **101**, 81.

[3] Y. Hou and A. H. Jayatissa, *Sens. Actuators B*, 2014, **204**, 310.

[4] F. Zhou, X. M. Zhao, Y. Q. Liu, C. G. Yuan and L. Li, Eur. *J. Inorg. Chem.*, 2008, **2008 (16)**, 2506.

[5] C. R. Xiong, A. E. Aliev, B. Gnade and K. J. Balkus, Jr, *ACS Nano*, **2 (2)**, 293.

[6] V. M. Mohan, B. Hu, W. L. Qiu and W. Chen, *J. Appl. Electrochem.*, 39, 2009, 2001.

[7] I. Raible, M. Burghard, U. Schlecht, A. Yasuda and T. Vossmeyer, *Sens. Actuators B*, 2005, **106**, 730.

[8] H. Y. Yu, B. H. Kang, U. H. Pi, C. W. Park and S. Y. Choi, *Appl. Phys. Lett.*, 2005, **86**, 253102.

[9] J. F. Liu, X. Wang, Q. Peng and Y. D. Li, *Adv. Mater.*, 2005, **17**, 764.

[10] V. Modafferi, G. Panzera, A. Donato, P.L. Antonucci, C. Cannilla, N. Donato, D. Spadaro and G. Neri, *Sens. Actuators B*, 2012, **163**, 61.

[11] Y. Vijayakumar, G. K. Mani, M. V. R. Reddy, J. B. B. Rayappan, *Ceram. Int.*, 2015, **41**, 2221.

[12] D. P. Volanti, A. A. Felix, M. O. Orlandi, G. Whitfield, D. J. Yang, E. Longo, H. L. Tuller and J. A. Varela, *Adv. Funct. Mater.*, 2013, **23**, 1759.

RSC Advances Accepted Manuscript

[13] M. Hjiri, L. E. Mir, S. G. Leonardi, A. Pistone, L. Mavilia and G. Neri, *Sens. Actuators B*, 2014, **196**, 413.

[14] C. W. Na, H. S. Woo, D. Kim and J. H. Lee, *Chem. Commun.*, 2011, **47**, 5148.

[15] C. W. Na, H. S. Woo and J. H. Lee, *RSC Adv.*, 2012, **2**, 414.

[16] N. singh, A. Ponzoni, R. K. Gupta, P. S. Lee and E. Comini, *Sens. Actuators B*, 2011, **160**, 1346.

[17] L. L. Wang, T. Fei, J. N. Deng, Z. Lou, R. Wang and T. Zhang, *J. Mater. Chem.*, 2012, **22**, 18111.

[18] Z. Lou, L. L. Wang, R. Wang, T. Fei and T. Zhang, *Solid State Electron.*, 2012, **76**, 91.

[19] J. Cao, T. Zhang, F. Li, H. Yang and S. Liu, *New J. Chem.*, 2013, **37**, 2031.

[20] G. D. Khuspe, S. T. Navale, D. K. Bandgar, R. D. Sakhare, M. A. Chougule and V. B. Patil, *Electron. Mater. Lett.*, 2014, **1**, 191.

[21] Q. Qi, P. P. Wang, J. Zhao, L. L. Feng, L. J. Zhou, R. F. Xuan, Y. P. Liu and G. D. Li, *Sens. Actuators B*, 2014, **194**, 440.

[22] Y. J. Chen, C. L. Zhu, X. L. Shi, M. S. Cao and H. B. Jin, *Nanotechnology*, 2008, **19**, 205603.

[23] M. Mashock, K. Yu, S. M. Cui, S. Mao, G. H. Lu and J. H. Chen, *ACS Appl. Mater. Interf.*, 2012, **4**, 4192.

[24] H. Zhang, J. C. Feng, T. Fei, S. Liu and T. Zhang, *Sens. Actuators B*, 2014, **190**, 472.

[25] V. Petkov, P. N. Trikalitis, E. S. Bozin, S. J. L. Billinge, T. Voget and M. G.

RSC Advances Accepted Manuscript

Kanatzidis, *J. Am. Chem. Soc.*, 2002, **124**, 10157.

[26] C. W. Na, H. S. Woo and J. H. Lee, *RSC Adv.*, 2012, **2**, 414.

[27] T. S. Wang, Q. S. Wang, C. L. Zhu, Q. Y. Ouyang, L. H. Qi, C. Y. Li, G. Xiao, P. Gao, Y. J. Chen, *Sens. Actuators B*, 2012, **171-172**, 256.

[28] L. X. Ling, R. G. Zhang, P. D. Han, B. J. Wang, *Fuel Process Technol.*, 2013, **16**, 222.

[29] Y. X. Qin, D. Y. Hua, M. Liu, *J Alloy. Comp.*, 2014, **587**, 227.

[30] R. A. Santen, M. Neurock, S. G. Shetty, *Chem. Rev.*, 2010, **110**, 2005.

[31] J. Liu, W. B. Guo, F. D. Qu, C. H. Feng, C. Li, L. H. Zhu, J. R. Zhou, S. P. Ruan and W. Y. Chen. *Ceram. Int.*, 2014, **40**, 6685.

[32] G. K. Mani and J. B. B. Rayappan. *Sens. Actuators B*, 2013, **183**, 459.

[33] A. Chatterjee, P. Bhattacharjee, N.K. Roy and P. Kumbhakar. *Int. J. Elec. Power*, 2013, **45**, 137.

[34] W. Jin, B. T. Dong, W. Chen, C. X. Zhao, L. Q. Mai and Y. Dai, *Sens. Actuators B*, 2010, **145**, 211.

[35] W. Jin, S. L. Yan, L. An, W. Chen, S. Yang, C. X. Zhao and Y. Dai, *Sens. Actuators B*, 2015, **206**, 284.

[36] L. L. Wang, Z. Lou, R. Wang, T. Fei and T. Zhang, *J. Mater. Chem.*, 2012, **22**, 12453.

RSC Advances Accepted Manuscript

Figure Captions

Fig. 1 The schematic of gas sensor fabricated by using alumina tube

Fig. 2 FESEM images of V_2O_5 nanowires (a) low-resolution image, (b) high-resolution image

Fig. 3 FESEM images of various V_2O_5 nanowires decorated with SnO_2 nanoparticles synthesized under various hydrothermal times: (a) Pure V_2O_5 nanowires, (b) 6h, (c) 12h, (d) 18h

Fig. 4 XRD patterns of pure V_2O_5 nanowires and the V_2O_5 nanowires decorated with SnO_2 nanoparticles prepared after various hydrothermal times

Fig. 5 (a) EDS pattern, (b) SEM image, EDS elemental mappings of (c) Sn element, (d) V element, (e) O element for the V_2O_5 nanowires decorated with SnO_2 nanoparticles prepared after hydrothermal times of 12 h

Fig. 6 TEM images of (a) pure V_2O_5 nanowires, and V_2O_5 nanowires decorated with SnO_2 nanoparticles prepared after hydrothermal times of (b) 6 h, (c) 12 h, (d) 18 h, (e) HRTEM images of SnO_2 decorated V_2O_5 nanowires prepared after hydrothermal time of 12 h

Fig. 7 Sensitivities of pure V_2O_5 nanowires and V_2O_5 nanowires decorated with SnO_2 nanoparticles prepared after hydrothermal times of 6 h, 12 h and 18 h to 10-1000 ppm ethanol at various operating temperatures: (a) 60 $^{\circ}$C, (b) 100 $^{\circ}$C, (c) 150 $^{\circ}$C, (d) 190 $^{\circ}$C, (e) 240 $^{\circ}$C, (f) 273 $^{\circ}$C, (g) 332 $^{\circ}$C, (h) 380 $^{\circ}$C

Fig. 8 (a) Sensitivity of the sensors based on SnO_2 nanoparticles and V_2O_5 nanowires decorated with SnO_2 nanoparticles prepared after hydrothermal time of 6, 12 h and 18

RSC Advances Accepted Manuscript

h to 1000 ppm concentration of ethanol gas at various temperature, (b) Sensitivity of SnO_2 nanoparticles, pure V_2O_5 nanowires and SnO_2 decorated V_2O_5 nanowires to 10-1000 ppm ethanol at 60 °C, (c) Sensitivity of the sensors based on V_2O_5 nanowires decorated with SnO_2 nanoparticles prepared after hydrothermal time of 12 h to different concentration of ethanol gas at room temperature

Fig. 9 (a) Selectivity of sensors based on V_2O_5 nanowires decorated with SnO_2 nanoparticles prepared after hydrothermal time of 12 h to 1000 ppm C_2H_5OH, CO_2, H_2O and NH_3 at different temperatures, (b) Stability of sensors based on SnO_2 decorated V_2O_5 nanowires prepared after hydrothermal time of 12 h to 1000 ppm ethanol at 332 °C

Fig. 10 Proposed ideal situation of oxygen adsorption depletion layer (a) before, (b) after SnO_2 decoration

Fig. 11 Proposed ideal band structure (a) before, (b) after contact between SnO_2 nanoparticles and V_2O_5 nanowires

Fig. 12 Proposed ideal path of electron transmission for (a) normal nanowires, (b) ultralong nanowires

RSC Advances Accepted Manuscript

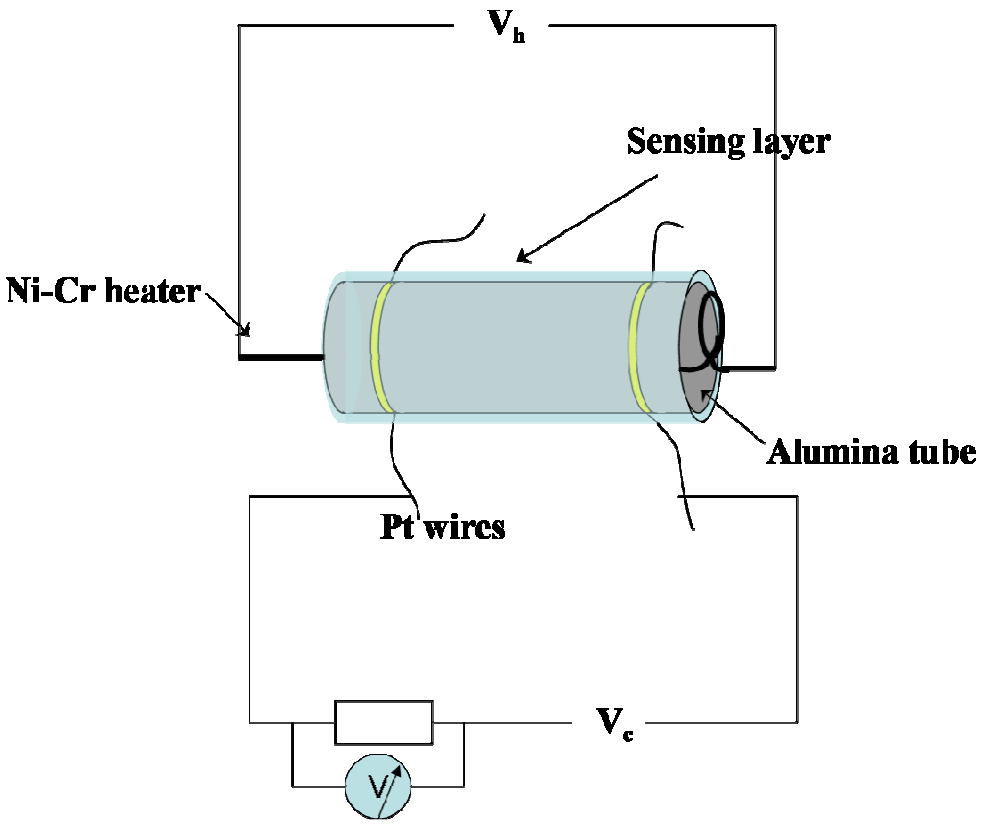

Fig. 1 The schematic of gas sensor fabricated by using alumina tube

RSC Advances Accepted Manuscript

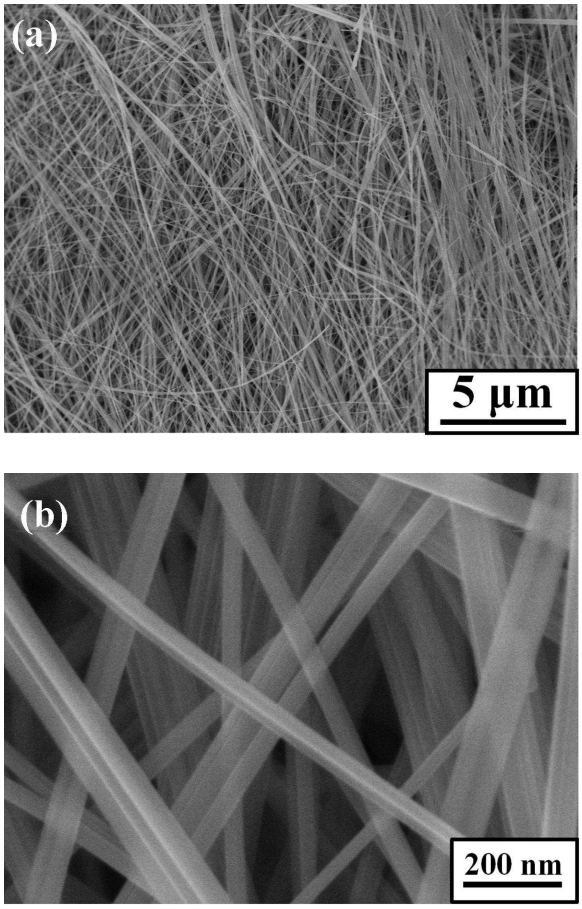

Fig. 2 FESEM images of V_2O_5 nanowires (a) low-resolution image, (b) high-resolution image

RSC Advances Accepted Manuscript

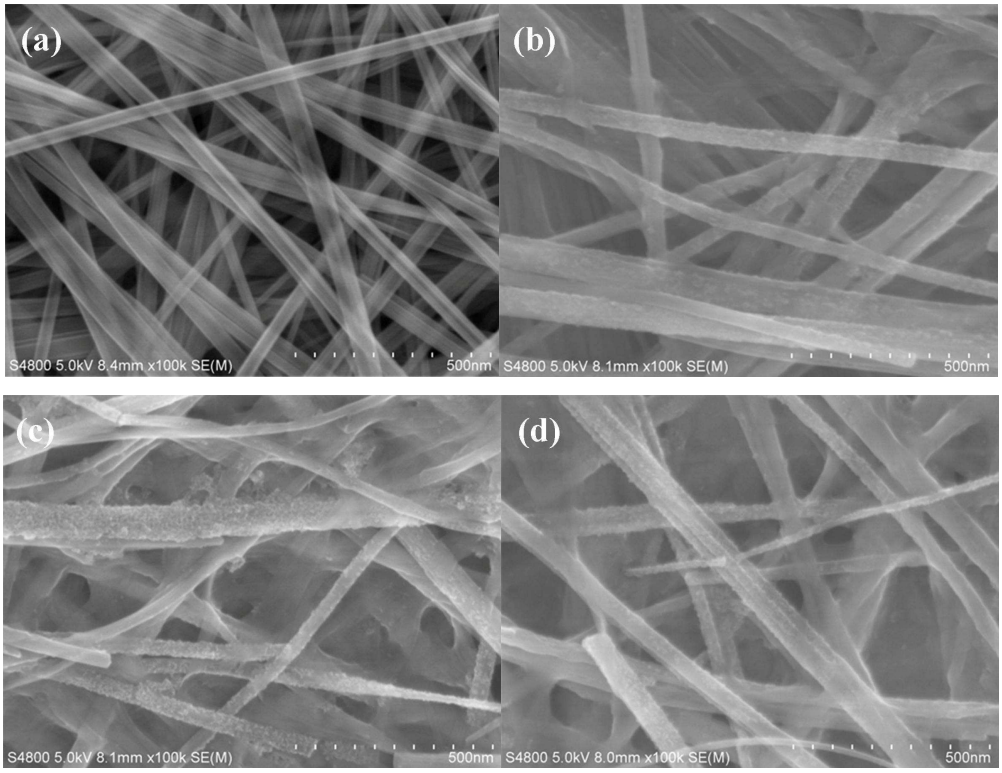

Fig. 3 FESEM images of various V_2O_5 nanowires decorated with SnO_2 nanoparticles synthesized under various hydrothermal times: (a) Pure V_2O_5 nanowires, (b) 6h, (c) 12h, (d) 18h

RSC Advances Accepted Manuscript

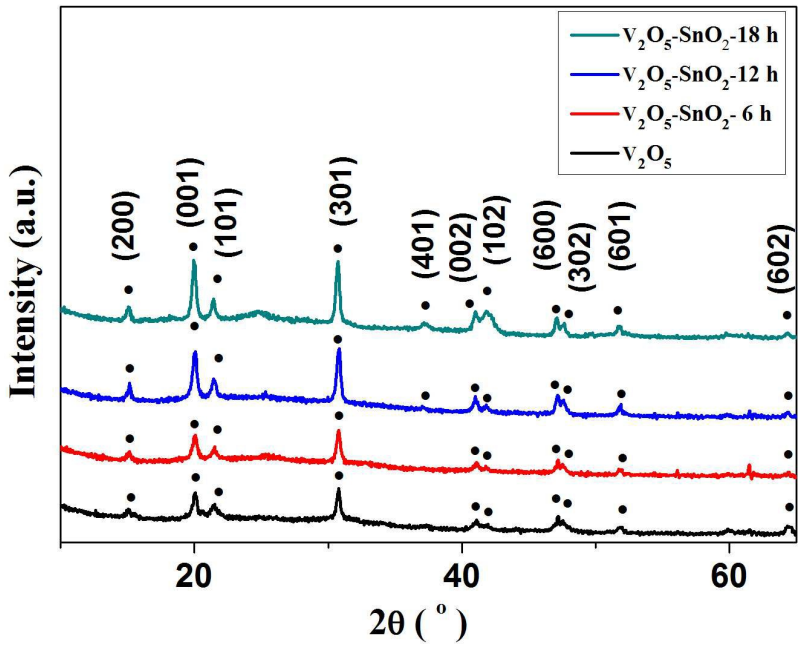

Fig. 4 XRD patterns of pure V_2O_5 nanowires and the V_2O_5 nanowires decorated with SnO_2 nanoparticles prepared after various hydrothermal times

RSC Advances Accepted Manuscript

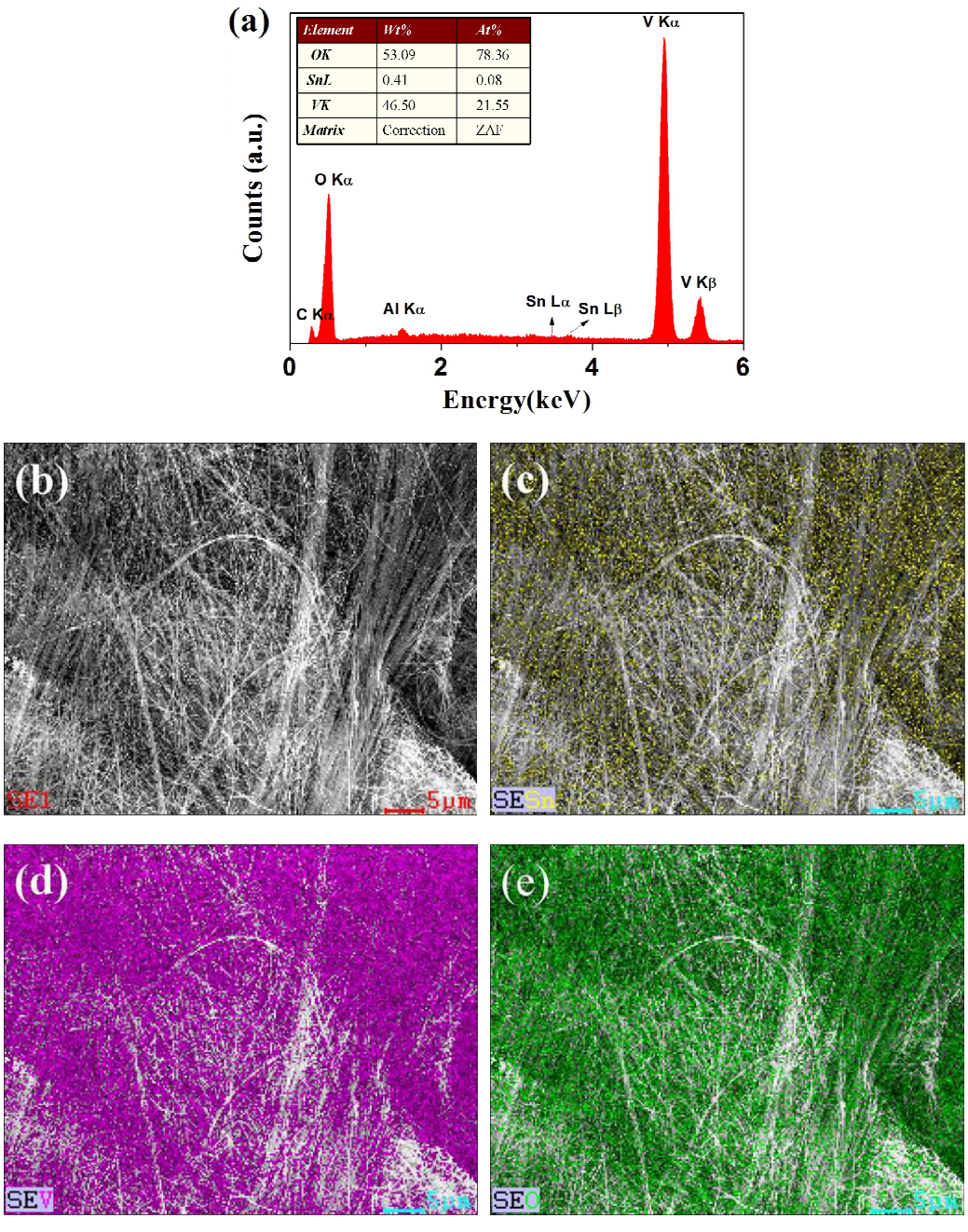

Fig. 5 (a) EDS pattern, (b) SEM image, EDS elemental mappings of (c) Sn element, (d) V element, (e) O element for the V_2O_5 nanowires decorated with SnO_2 nanoparticles prepared after hydrothermal times of 12 h

RSC Advances Accepted Manuscript

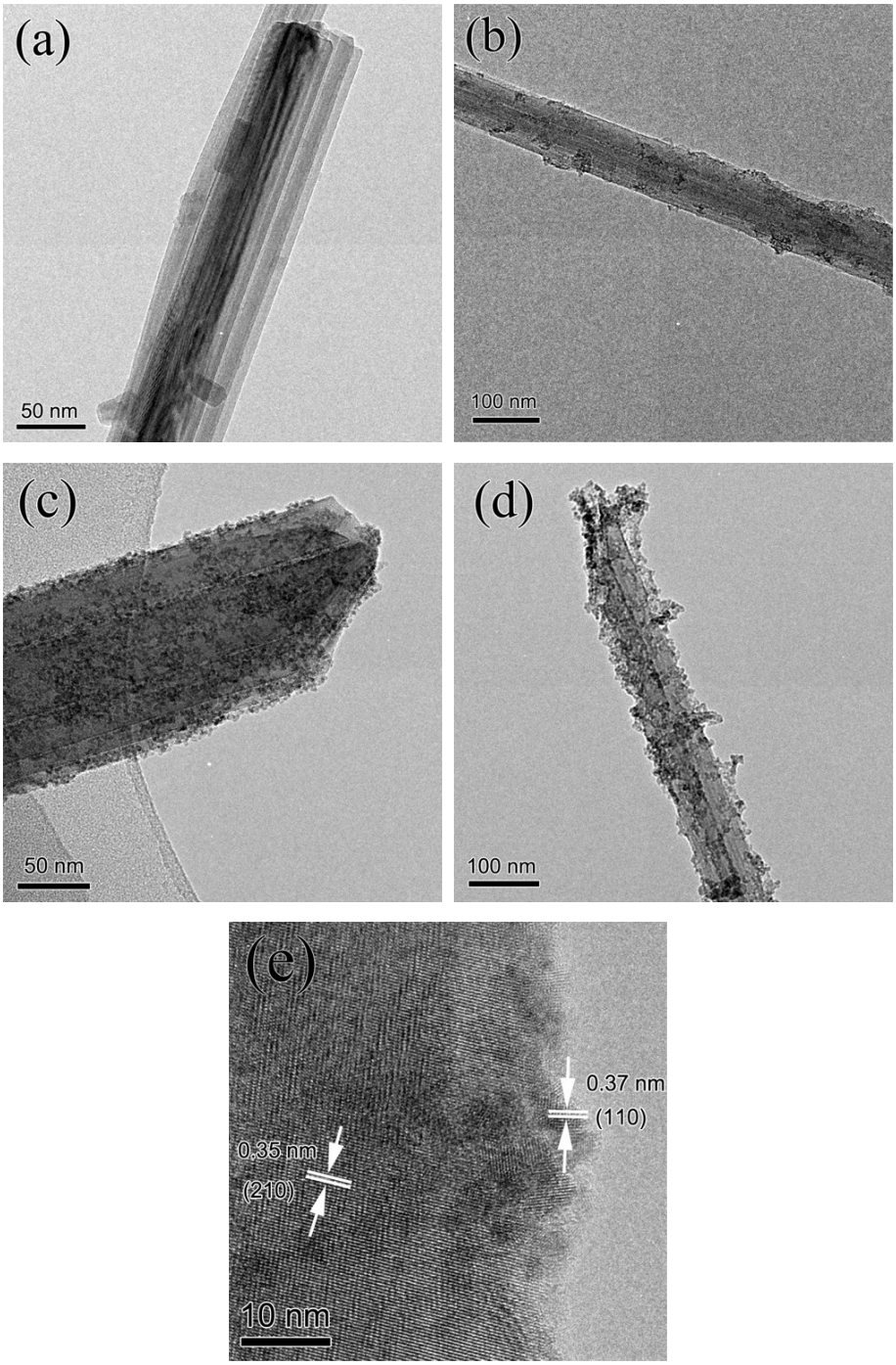

Fig. 6 TEM images of (a) pure V_2O_5 nanowires, and V_2O_5 nanowires decorated with SnO_2 nanoparticles prepared after hydrothermal times of (b) 6 h, (c) 12 h, (d) 18 h, (e) HRTEM images of SnO_2 decorated V_2O_5 nanowires prepared after hydrothermal time of 12 h

RSC Advances Accepted Manuscript

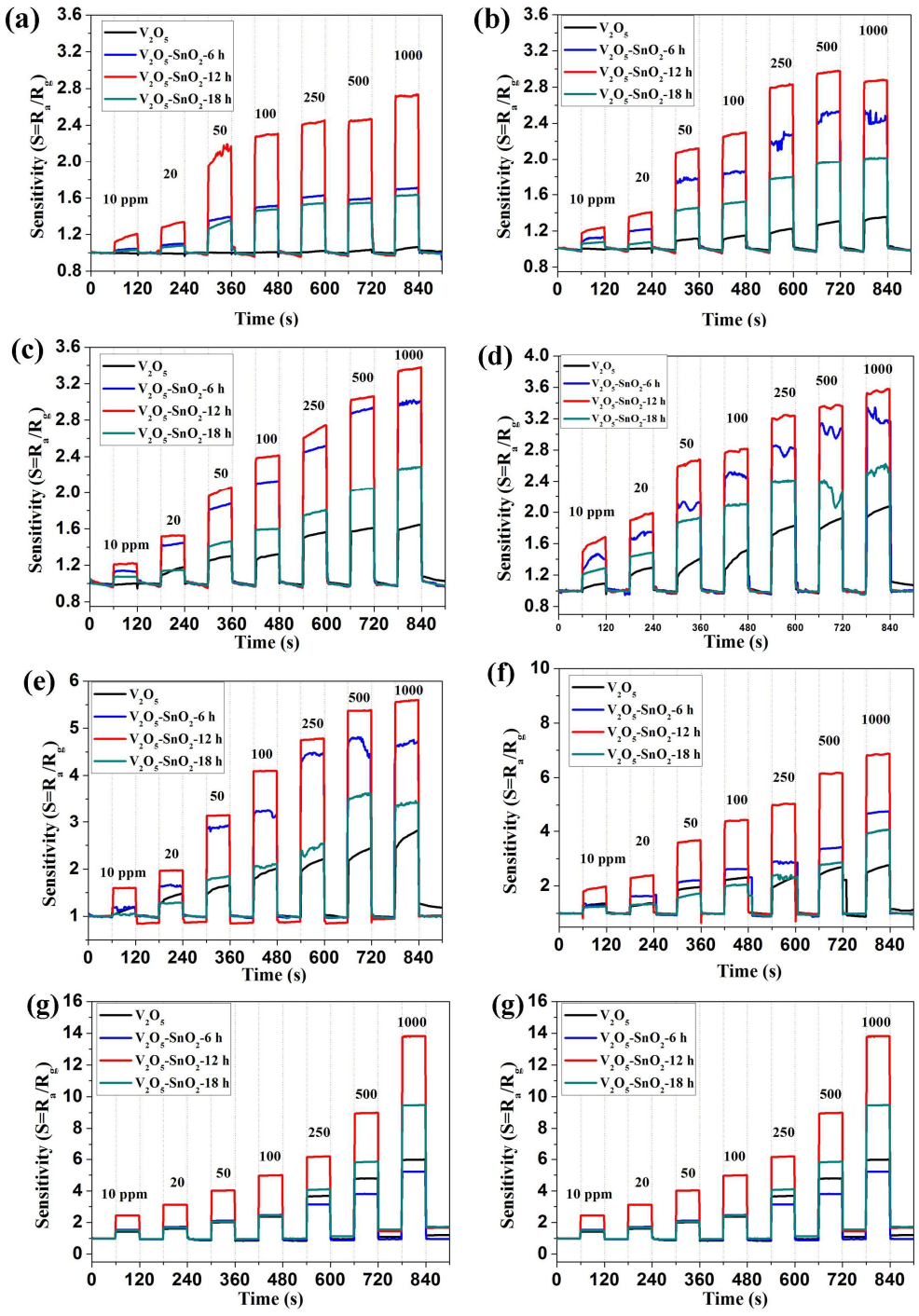

Fig. 7 Sensitivities of pure V_2O_5 nanowires and V_2O_5 nanowires decorated with SnO_2 nanoparticles prepared after hydrothermal times of 6 h, 12 h and 18 h to 10-1000 ppm ethanol at various operating temperatures: (a) 60 ˚C, (b) 100 ˚C, (c) 150 ˚C, (d) 190 ˚C, (e) 240 ˚C, (f) 273 ˚C, (g) 332 ˚C, (h) 380 ˚C

RSC Advances Accepted Manuscript

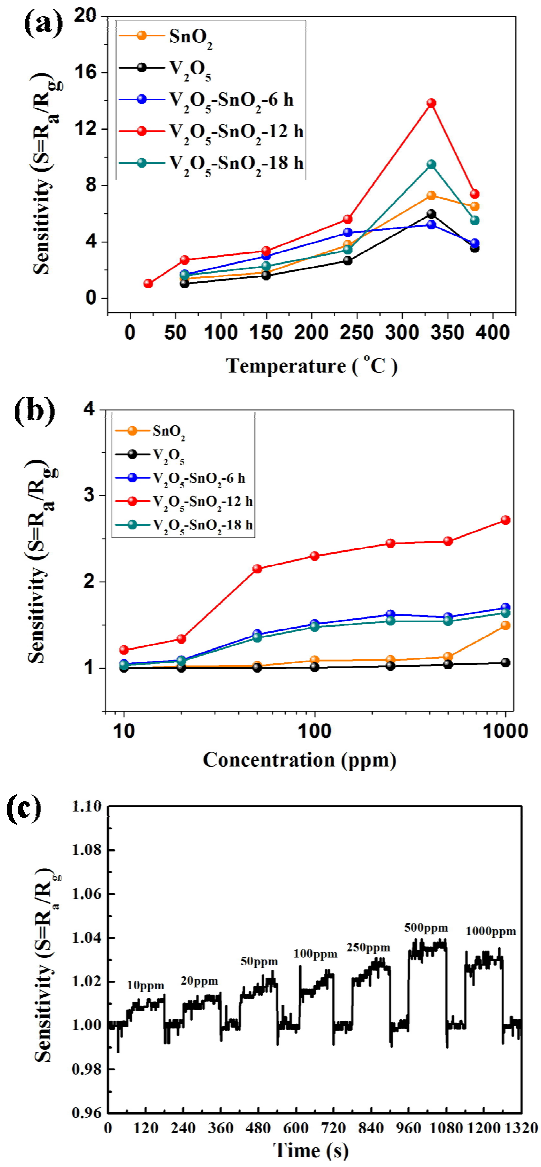

Fig. 8 (a) Sensitivity of the sensors based on SnO_2 nanoparticles and V_2O_5 nanowires decorated with SnO_2 nanoparticles prepared after hydrothermal time of 6, 12 h and 18 h to 1000 ppm concentration of ethanol gas at various temperature, (b) Sensitivity of SnO_2 nanoparticles, pure V_2O_5 nanowires and SnO_2 decorated V_2O_5 nanowires to 10-1000 ppm ethanol at 60 °C, (c) Sensitivity of the sensors based on V_2O_5 nanowires decorated with SnO_2 nanoparticles prepared after hydrothermal time of 12 h to different concentration of ethanol gas at room temperature

RSC Advances Accepted Manuscript

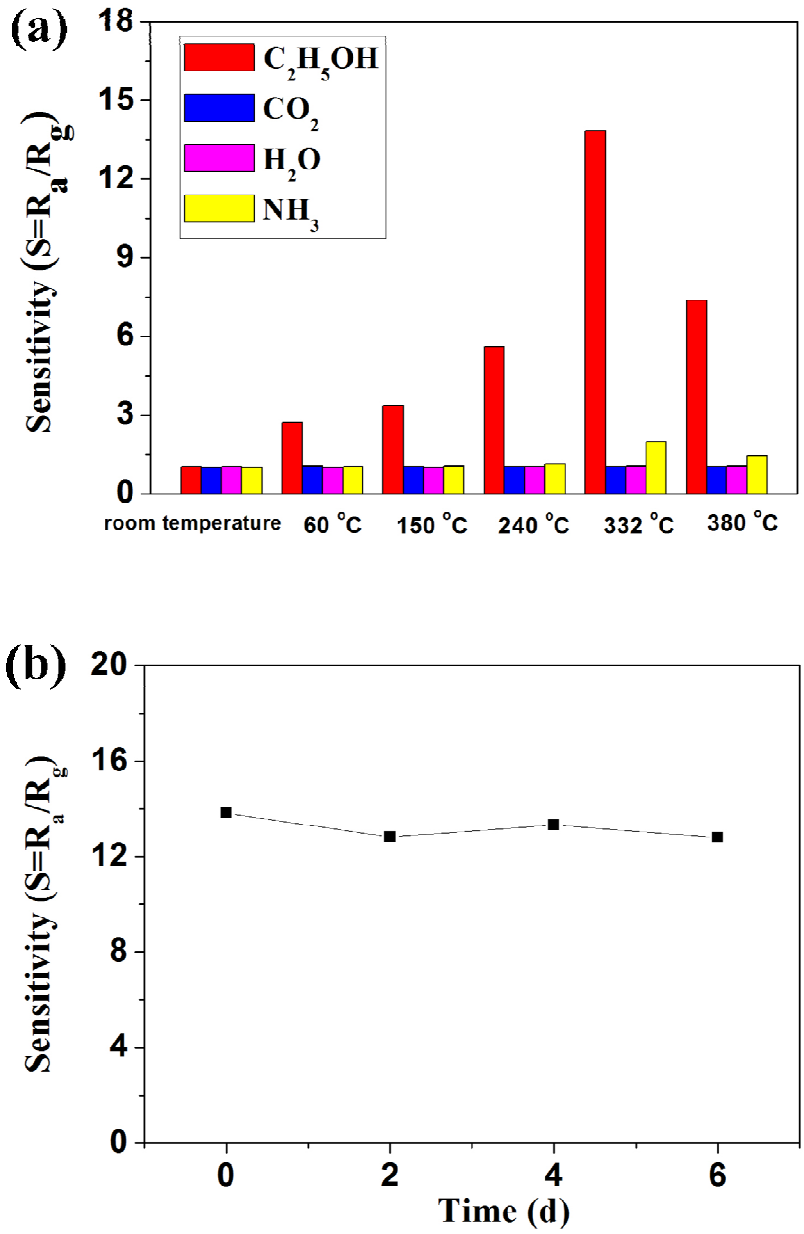

Fig. 9 (a) Selectivity of sensors based on V_2O_5 nanowires decorated with SnO_2 nanoparticles prepared after hydrothermal time of 12 h to 1000 ppm C_2H_5OH, CO_2, H_2O and NH_3 at different temperatures, (b) Stability of sensors based on SnO_2 decorated V_2O_5 nanowires prepared after hydrothermal time of 12 h to 1000 ppm ethanol at 332 ˚C

RSC Advances Accepted Manuscript

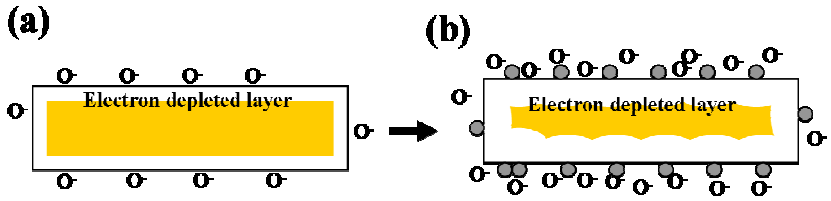

Fig. 10 Proposed ideal situation of oxygen adsorption depletion layer (a) before, (b) after SnO_2 decoration

RSC Advances Accepted Manuscript

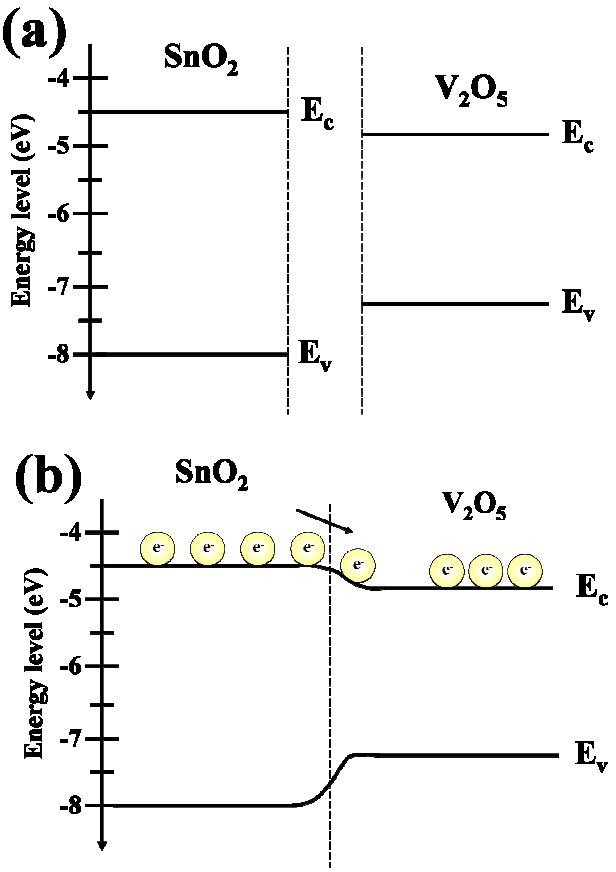

Fig. 11 Proposed ideal band structure (a) before, (b) after contact between SnO_2 nanoparticles and V_2O_5 nanowires

RSC Advances Accepted Manuscript

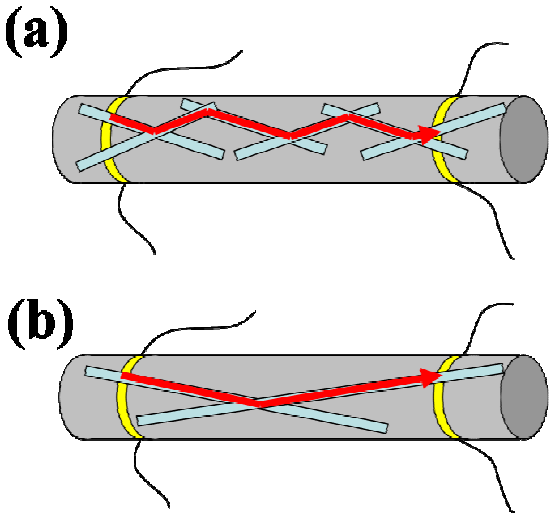

Fig. 12 Proposed ideal path of electron transmission for (a) normal nanowires, (b) ultralong nanowires

RSC Advances Accepted Manuscript